Recurrent fusion of *MYB* and *NFIB* transcription factor genes in carcinomas of the breast and head and neck

Marta Persson[a,1], Ywonne Andrén[a,1], Joachim Mark[b], Hugo M. Horlings[c], Fredrik Persson[a], and Göran Stenman[a,2]

[a]Lundberg Laboratory for Cancer Research, Department of Pathology, the Sahlgrenska Academy at University of Gothenburg, SE-413 45 Gothenburg, Sweden; [b]Department of Pathology, Central Hospital, SE-541 85 Skövde, Sweden; and [c]Division of Experimental Therapy, The Netherlands Cancer Institute, 1066CX, Amsterdam, The Netherlands

Edited by George Klein, Karolinska Institute, Stockholm, Sweden, and approved September 2, 2009 (received for review August 11, 2009)

The transcription factor gene *MYB* was identified recently as an oncogene that is rearranged/duplicated in some human leukemias. Here we describe a new mechanism of activation of *MYB* in human cancer involving gene fusion. We show that the t(6;9)(q22–23;p23–24) translocation in adenoid cystic carcinomas (ACC) of the breast and head and neck consistently results in fusions encoding chimeric transcripts predominantly consisting of *MYB* exon 14 linked to the last coding exon(s) of *NFIB*. The minimal common part of *MYB* deleted as the result of fusion was exon 15 including the 3′-UTR, which contains several highly conserved target sites for miR-15a/16 and miR-150 microRNAs. These microRNAs recently were shown to regulate *MYB* expression negatively. We suggest that deletion of these target sites may disrupt repression of *MYB* leading to overexpression of *MYB-NFIB* transcripts and protein and to activation of critical *MYB* targets, including genes associated with apoptosis, cell cycle control, cell growth/angiogenesis, and cell adhesion. Forced overexpression of miR-15a/16 and miR-150 in primary fusion-positive ACC cells did not significantly alter the expression of *MYB* as compared with leukemic cells with *MYB* activation/duplication. Our data indicate that the *MYB-NFIB* fusion is a hallmark of ACC and that deregulation of the expression of *MYB* and its target genes is a key oncogenic event in the pathogenesis of ACC. Our findings also suggest that the gain-of-function activity resulting from the *MYB-NFIB* fusion is a candidate therapeutic target.

chromosome translocation | fusion oncogene | miRNA | adenoid cystic carcinoma

Fusion genes are potent oncogenes resulting from chromosome rearrangements, in particular translocations. Most fusion genes identified thus far have been in hematological disorders and mesenchymal neoplasms, and only a few have been found in carcinomas (1). This paucity probably results from an inability to discover these rearrangements rather than from a true lack of such genes in carcinomas. The recent discovery that the majority of prostate cancers harbor *ETS* gene fusions (2) is in line with this reasoning. Finding as yet unidentified fusion oncogenes in other carcinomas could provide important insights into the molecular pathogenesis of these cancers and also might facilitate the development of new targeted therapies.

We previously have identified a recurrent and tumor-specific t(6;9)(q22–23;p23–24) translocation in adenoid cystic carcinoma (ACC) of the head and neck (3). The translocation has been found as the sole cytogenetic anomaly in several cases, indicating that it is a primary rearrangement in this carcinoma.

ACC has been known as a histologically distinctive neoplasm for nearly 150 years. It is among the most common carcinomas of the salivary glands (4) but also may arise in other exocrine glands, such as in the breast, and in the cervix, vulva, and tracheobronchial tree (5). ACC usually is an aggressive, although slowly growing, cancer with a long-term poor prognosis. Most patients (80–90%) with ACC of the head and neck die within 10–15 years after diagnosis. However, despite extensive studies, the molecular pathogenesis of this carcinoma is poorly understood. Here we show that the t(6;9)(q22–23;p23–24) translocation in ACC consistently results in a fusion of the *MYB* oncogene to the transcription factor gene *NFIB*. The fact that all ACCs analyzed expressed the *MYB*-fusion, irrespective of whether they were derived from the salivary glands, lacrimal glands, ceruminal glands, or breast, indicates that the *MYB-NFIB* fusion is a hallmark of this tumor type.

Results and Discussion

We performed cytogenetic and spectral karyotype analyses of primary and metastatic ACCs of the head and neck and identified a t(6;9) translocation in 6 of 6 cases (Fig. 1*A* and Table 1). Using FISH and a panel of yeast artificial chromosome (YAC) clones derived from 9p23–24 (6), we found that YAC-912E9 spanned the 9p23–24 breakpoint in an ACC with a t(6;9). This YAC contains *NFIB*, a member of the human nuclear factor I (*NFI*) gene family of transcription factors, as the only named gene (6). NFI proteins contain DNA binding and dimerization domains in their N-termini and proline-rich, transactivation domains in their C-termini (7). Interestingly, we previously have identified *NFIB* as a recurrent fusion partner to *HMGA2* in benign pleomorphic salivary gland adenomas with t(9;12) translocations (6, 8).

Initial FISH mapping of the 6q22–24 translocation breakpoint revealed that it is located proximal to the *PLAGL1* locus in 6q24–25 (9). Further analysis using a panel of bacterial artificial chromosome (BAC) clones derived from 6q22–24 (available on request) revealed that the breakpoint is located within a 1.1-Mb region containing *MYB*, *AHI1*, *PDE7B*, *FAM54A*, and *BCLAF*. Based on the known functions of these genes and their previous involvement in cancer, we reasoned that the *MYB* oncogene might be a likely target of the t(6;9). *MYB* encodes a transcription factor with an N-terminal DNA binding domain, a centrally located transcription activation domain, and a C-terminal negative regulatory domain (10, 11). MYB plays an important role in the control of cell proliferation, apoptosis, and differentiation, is highly expressed in immature, proliferating cells, and is down-regulated as cells become more differentiated (10, 11). Recent studies also have demonstrated that *Myb* is expressed in the mouse submandibular gland at embryonic day E14.5 (12), suggesting a role for *Myb* in salivary gland development. To test the possibility that *MYB* is the target gene in 6q22–24, we

Author contributions: M.P., Y.A., F.P., and G.S. designed research; M.P., Y.A., and F.P. performed research; J.M., H.M.H., and G.S. contributed new reagents/analytic tools; M.P., Y.A., F.P., and G.S. analyzed data; and M.P., Y.A., F.P., and G.S. wrote the paper.

The authors declare no conflict of interest.

This article is a PNAS Direct Submission.

Data deposition: The sequences reported in this paper have been deposited in the GenBank database (accession nos. FJ969915, FJ969916, and FJ969917).

[1]M.P. and Y.A. contributed equally to this work.

[2]To whom correspondence should be addressed at: Department of Pathology, Sahlgrenska University Hospital, SE-413 45 Gothenburg, Sweden. E-mail: goran.stenman@llcr.med.gu.se.

This article contains supporting information online at www.pnas.org/cgi/content/full/0909114106/DCSupplemental.

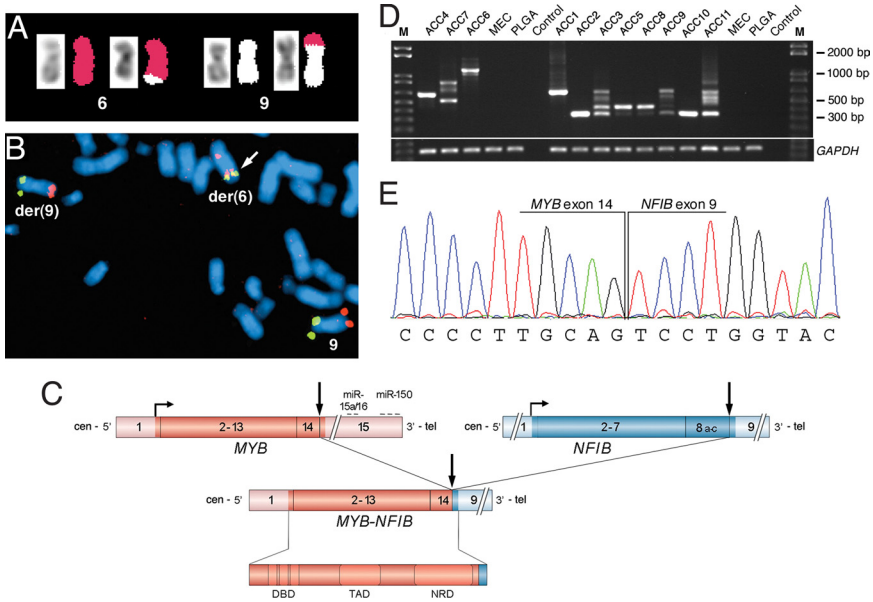

Fig. 1. The t(6;9) translocation in ACC results in a *MYB-NFIB* fusion. (*A*) Partial SKY-karyotype showing the reciprocal t(6;9) translocation in ACC6. DAPI-banded chromosomes 6 and 9 are shown on the left. (*B*) Dual-color FISH analysis of a t(6;9)-positive tumor (ACC6) using the *NFIB*-specific YAC-912E9 (*green signals*) and BAC clones RP11–104D9 and RP11–349J5 containing the 5′ part of *MYB* and its flanking sequences (*red signals*). Chromosome 6 is identified by a red alpha-satellite probe and chromosome 9 by a red telomere probe on the q-arm. Note the presence of the *MYB-NFIB* fusion gene on the der (6) marker (*fused red/green signals marked by arrow*). (*C*) Schematic illustration depicting the *MYB* and *NFIB* genes as well as the *MYB-NFIB* fusion gene (coding exons are shown in darker red and blue) and the resulting fusion protein. Translocation breakpoints are shown by vertical arrows, and miRNA binding sites for miR-15a/16 and miR-150 in the 3′ UTR of *MYB* are indicated. DBD, DNA binding domain; NRD, negative regulatory domain; TAD, transactivation domain. (*D*) RT-PCR analyses of *MYB-NFIB* fusion transcripts using primers located in *MYB* exons 5/6 and *NFIB* exon 9 (ACC4, -7, -6) and in *MYB* exon 14 and *NFIB* exon 9 (ACC1, -2, -3, -5, - 8–11). Also shown are size markers (M), non-ACC tumors (MEC and PLGA), and negative control. (*E*) Partial chromatogram showing the *MYB-NFIB* junction (*vertical lines*) and the nucleic acid sequence of the chimeric transcript with an in-frame fusion of *MYB* exon 14 to *NFIB* exon 9.

performed FISH experiments using the *NFIB*-containing YAC-912E9 in combination with 2 sets of BAC clones (RP11–104D9 and RP11–349J5 or RP11–63K22 and RP11–258C9) containing the 5′ parts of *MYB* and its flanking sequences. FISH analysis of a t(6;9)-positive ACC revealed a fusion signal on the derivative chromosome 6 consisting of the 5′ part of *MYB* linked to *NFIB* sequences (Fig. 1*B*). RT-PCR analysis of tumor RNA prepared from this case confirmed the expression of *MYB-NFIB* hybrid transcripts (Fig. 1 *C* and *D*).

To determine whether the *MYB-NFIB* fusion is a recurrent event in ACC, we screened tumor RNAs from 10 additional primary and metastatic ACCs, including 6 head and neck-derived and 4 breast-derived tumors (Table 1). RT-PCR analysis revealed *MYB-NFIB* fusion transcripts in all ACCs but not in 25 different non-ACC tumor samples (Fig. 1*D*). Reciprocal *NFIB-MYB* fusion products were detected in only 3 of 8 ACCs, indicating that nonreciprocal, complex 6;9-rearrangements also exist.

Because of alternative splicing and variable breakpoints in *MYB* and *NFIB*, we identified and characterized at least 11 *MYB-NFIB* transcript variants (supporting information (SI) Table S1). Chimeric transcripts consisting of *MYB* exon 14 linked

Table 1. Clinical-pathological and genetic data on 11 ACCs

Tumor	Sex/age (years)	Size (cm)	Tumor site	t(6;9)	*MYB-NFIB* fusion	Clinical outcome
ACC1	F/47	3.2	Submandibular	yes	+	NED 14 years
ACC2	F/77	1.4	Submandibular	yes	+	NED 1 year
ACC3	M/38	2.3	Parotid	NDA	+*	NED 9 years
ACC4	F/34	NDA	Maxilla	yes	+†	Lymph node mets 0 years, lung mets 4 years, AWD 8 years
ACC5	M/77	4	Pelvic bone met (primary tumor nasal cavity)	yes	+*	LR 3, 5, 8 years, lymph node mets 5, 9 years, pelvic bone mets 5 years, lung mets 9 years, TRD 9 years
ACC6	M/29	1	Lacrimal	yes	+*,†	NED 5 years
ACC7	F/45	NDA	Auditory meatus	yes	+†	NED 4 years
ACC8	F/41	2.4	Breast	NDA	+*	NED 15 months
ACC9	F/55	3.5	Breast	NDA	+*	NED 21 months
ACC10	F/78	2.1	Breast	NDA	+	DOC 3 months
ACC11	F/60	2.6	Breast	NDA	+*	NED 8.5 years

Abbreviations: DOC, dead of other causes; LR, local recurrence; mets, metastases; NED, no evidence of disease; NDA, no data available; TRD, tumor-related death; AWD, alive with disease.

*Contains *MYB-NFIB* fusion transcripts both with and without the alternatively spliced *MYB* exon 9a.

†Express reciprocal *NFIB-MYB* fusion transcripts.

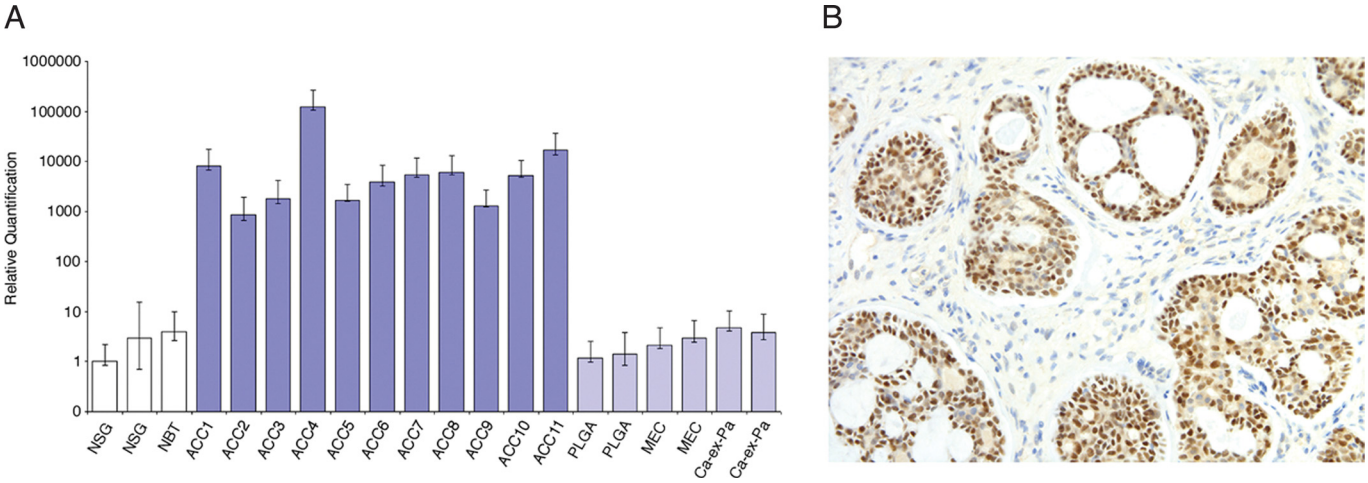

Fig. 2. The t(6;9) translocation in ACC results in overexpression of *MYB-NFIB* mRNA and protein. (*A*) Q-PCR analyses of the expression of *MYB* in ACC1–11 (*dark blue bars*) and in non-ACC tumors (PLGA, MEC, and Ca-ex-PA) (*light blue bars*) compared with normal salivary gland (NSG) and breast (NBT) tissues (*white bars*). (*B*) Immunostaining of the MYB-NFIB fusion protein in a primary t(6;9)-positive cribriform type of ACC (ACC2). Note the strong nuclear staining of tumor cells and the absence of staining in stromal cells.

to *NFIB* exons 8c or 9 predominated (Fig. 1 *C* and *E*), indicating that most breakpoints had occurred in *MYB* intron 14 and in *NFIB* intron 8 (Fig. 1*C*). The majority of transcripts were the result of expression of the alternatively spliced *NFIB* exons 8a, 8a alt, 8b, and/or 8c. Of the 11 ACCs, 6 also expressed chimeric transcripts both with and without the alternatively spliced *MYB* exon 9a (13).

To study the consequences of the *MYB-NFIB* fusion on the expression of *MYB*, we performed quantitative real-time PCR (Q-PCR) on ACCs using a TaqMan probe covering exons 1–2. *MYB* indeed was highly overexpressed in ACC relative to normal salivary gland and breast tissues and to 3 other types of salivary gland carcinomas ($P = 0.0001$) (Fig. 2*A*). In contrast, a TaqMan probe covering *MYB* exons 14–15 revealed expression levels that were significantly reduced compared with *MYB* exons 1–2 ($P = 0.001$) (Table S2), consistent with disruption of the 3′ part of *MYB* as a consequence of gene fusion. These experiments clearly demonstrate that the increased expression of *MYB* is not caused by expression of the non-rearranged *MYB* allele. High-level overexpression of MYB at the protein level also was confirmed by immunostaining (Fig. 2*B*) of 5 primary ACCs.

The molecular mechanism by which *MYB* is activated by the t(6;9) is previously undescribed. The minimal common part of *MYB* lost as the result of the fusions was the 3′ end including exon 15, which encodes the last 38 amino acids of the MYB protein, and the minimal common part of *NFIB* linked to *MYB* was exon 9 (Fig. 1*C*), which encodes the last 5 amino acids (SWYLG) of the NFIB protein. Although it has been suggested that these 5 amino acids are critical for the proper function of the transcription factor (14), their contribution to the pathogenesis of ACC is expected to be limited. Nor do our results indicate that the majority of fusions disrupt the C-terminal, leucine-rich negative regulatory domain of *MYB* encoded by exons 10–13 (10, 15–17). Instead, our data raise the question of whether *MYB* may be deregulated as a result of loss of the 3′ end of the gene including several microRNA (miRNA) binding sites in the 3′ UTR. There are at least 2 highly conserved miR-15a/16 and 3 miR-150 miRNA target sites in the 3′ UTR of *MYB* (Fig. 1*C*). Recent studies have demonstrated that *MYB* is a major target of these miRNAs and that they negatively regulate *MYB* expression through these binding sites (18–21).

To test the hypothesis that deletion of these target sites through gene fusion may disrupt the repression of *MYB*, we overexpressed miR-15a, miR-16, and miR-150 in ACC cells, as well as in a T-cell acute lymphoblastic leukemia (T-ALL) cell line (MOLT-4) that overexpresses *MYB* because of a duplication of the *MYB* locus (22), and assayed their effects on the expression of *MYB*. In the absence of t(6;9)-positive, authentic ACC cell lines (23) we used primary cultured fusion-positive ACC cells. Transfection of MOLT-4 cells with premiR-15a/16 and premiR-150 resulted in a ≈30% down-regulation of *MYB* mRNA expression after 45 h, whereas transfection of primary ACC cells did not alter the expression levels of *MYB* significantly (Fig. 3*A*). Transfection of primary ACC cells with a Cy3-labeled premiR-negative control resulted in a transfection efficiency of more than 95% (Fig. 3*B*). The observed reduction in *MYB* mRNA expression in the control T-ALL cells is comparable to previously published data (20). Expression analysis of miR-15a/16 and miR-150 revealed that they indeed are expressed in both ACC and in normal salivary gland and breast tissues; miR-15a/16 were overexpressed in ACC as compared with normal glandular tissues, whereas the expression of miR-150 was lower in ACC than in normal glandular tissues (Fig. S1). Taken together, these data support our hypothesis that deletion of miRNA binding sites in the 3′ UTR of *MYB* through gene fusion may disrupt the repression of *MYB* by miRNAs. We cannot, however, exclude the possibility that loss of parts of the *MYB* negative regulatory domain or of sequences in the 3′ UTR of *NFIB* also may contribute to the deregulation of *MYB* expression. Interestingly, recent studies have shown that the expression of *HMGA2*, another oncogene frequently activated by chromosomal translocations, also is deregulated by the loss of negatively regulating Let-7 miRNA target sites in the 3′ UTR of *HMGA2* as a consequence of gene fusions (24, 25). In a small subset of these cases, the activation is the result of fusions of the last 5 amino acids of the NFIB protein to the DNA binding domains of *HMGA2* (6, 8), the same part of *NFIB* that is fused to *MYB* in ACC. Our findings thus may represent a second example of miRNA-directed repression of an oncogene activated by chromosomal translocations. Together with recent findings of duplications of *MYB* or t(6;7)(q23;q34) translocations placing an intact *MYB* locus in the vicinity of *TCRB* regulatory sequences in T-ALL (22, 26), the present results further emphasize the significance of *MYB* as an important human oncogene.

To gain insight into the molecular consequences of constitutive, high-level expression of the *MYB-NFIB* fusion, we analyzed the expression of 16 *MYB* target genes (11, 27) in ACC relative

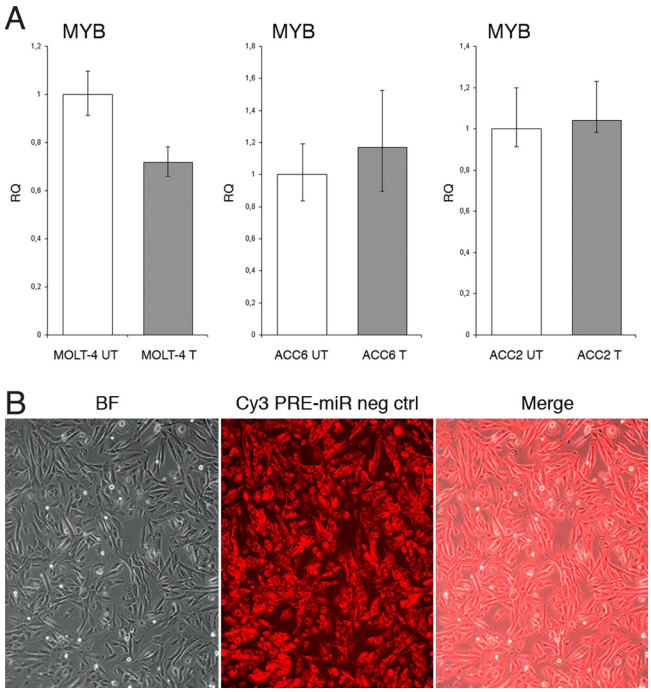

Fig. 3. Forced overexpression of miR-15a, miR-16, and miR-150 in T-ALL and primary ACC cells. (*A*) Q-PCR analyses of *MYB* mRNA expression in MOLT-4 cells with duplication/activation of *MYB* and in *MYB-NFIB*–expressing primary ACC2 and -6 cells after transfection with a pool of premiR-15a, premiR-16, and premiR-150 oligos. The data represent the average of at least 3 independent experiments. T, transfected; UT, untransfected. (*B*) Transfection of primary ACC6 cells with a Cy3-labeled premiR negative control shows a transfection efficiency of more than 95%. BF, bright field.

to normal salivary gland tissue. Analysis of a panel of 7 ACCs revealed unequivocal overexpression of 14 *MYB* target genes associated with apoptosis (*API5*, *BCL2*, *BIRC3*, *HSPA8*, *SET*), cell cycle control (*CCNB1*, *CDC2*, *MAD1L1*), cell growth/angiogenesis (*MYC*, *KIT*, *VEGFA*, *FGF2*, *CD53*), and cell adhesion (*CD34*) (Fig. S2). In contrast, *CBX4* and *TFEC* were not consistently highly overexpressed in ACC as compared with normal salivary gland tissue. Using a bioinformatic approach, we also confirmed overexpression of *API5*, *BCL2*, *CDC2*, and *MYC* and of *BCL2* and *CDC2*, respectively, in 2 independent ACC gene-expression array data sets (28, 29). Overexpression of *KIT* has also been shown previously to occur in the majority of ACCs (4).

In summary, our findings suggest that deregulation of the expression of *MYB* and its target genes is a key oncogenic event in the pathogenesis of ACC. The fact that all ACCs analyzed expressed the *MYB* fusion, irrespective of whether they were derived from the salivary glands, lacrimal glands, ceruminal glands of the ear, or breast, indicate that the fusion is a hallmark of this tumor type. Defining the molecular mechanism underlying the activation of *MYB* by the t(6;9) and the potential contribution of *NFIB* will provide new information about the role of these transcription factors in normal and transformed cells. Our findings also suggest new possibilities for diagnosis and treatment of ACC and identify the gain-of-function activity resulting from the *MYB-NFIB* fusion as a candidate therapeutic target.

Materials and Methods

Tumor Material. Fresh ACC samples from 11 patients were obtained at the time of surgery. Of these tumors, 10 represented primary lesions, and 1 was a pelvic bone metastasis; 7 tumors were derived from the head and neck region, and 4 were derived from the breast. Histopathological re-examination of the tumors confirmed the diagnosis of ACC in all cases. The clinical-pathological characteristics of all tumors are shown in Table 1. For Q-PCR analysis we used fresh-frozen tumor tissue from 25 additional non-ACC salivary gland carcinomas [mucoepidermoid carcinomas (MEC), polymorphous low-grade adenocarcinomas, (PLGA), carcinoma ex pleomorphic adenoma (Ca-ex-Pa)] and invasive ductal carcinomas of the breast. The T-ALL cell line MOLT-4 (ATCC No. CRL-1582) was used for transfection of miRNAs.

The study was approved by the regional ethics committee in Gothenburg, Sweden (D-no: 178–08).

Cytogenetic, Spectral Karyotype, and Fluorescence in Situ Hybridization (FISH) Analyses. Primary cultures were established from fresh, unfixed tumor specimens of 6 ACCs (ACC1–2 and -4–7) as previously described (3, 30). Chromosome preparations were made from primary cultures or early-passage cells. Chromosomes were G-banded and analyzed using standard procedures. Spectral karyotype analysis was performed on all 6 cases as previously described (30). FISH analysis was performed on metaphase chromosomes (30) using a series of BAC clones derived from 6q22–24 (available on request) as well as a panel of YAC clones derived from 9p23–24 (6). Fluorescence signals were digitalized, processed, and analyzed using the CytoVision™ image analysis system (Applied Imaging International Ltd.).

RT-PCR and Nucleotide Sequence Analyses. Total RNA was extracted from frozen tumor tissue and normal salivary gland using the TRIzol reagent (Invitrogen). DNase-treated (DNA-free™; Ambion) total RNA was converted subsequently to cDNA using the SuperScript™ First-Strand Synthesis System (Invitrogen) according to the manufacturer's manual. As a control for intact RNA and cDNA, RT-PCR reactions for expression of *GAPDH* were performed on all cDNAs. The *MYB-NFIB* fusion transcripts were amplified by direct or nested PCR. The first-round PCR was carried out using the *MYB* primers MYB-697F-5′GGCAGAAATCGCAAAGCTAC3′ (located in exon 5) or MYB-1693F-5′GCAGGATGTGATCAAACAGG3′ (located in exon 12) and the *NFIB* primer NFIB-2078R-5′CTATTTCCCAGCGGACTTCA3′ (located in exon 9). The second-round PCR was performed using the *MYB* primers MYB-876F-5′CTCCGCCTACAGCTCAACTC3′ (located in exon 6) or MYB-1925F-5′GCACCAGCATCAGAAGATGA3′ (located in exon 14) and the *NFIB* primer NFIB-1952R-5′GTGCTGCAATTGCTGGTCTA3′ (located in exon 9). PCR products were gel-purified and sequenced using an ABI PRISM 310 Genetic Analyzer (Applied Biosystems). The resulting sequences were analyzed using the BLAST tool provided by the National Center for Biotechnology Information (http://www.ncbi.nlm.nih.gov).

Quantitative Real-Time PCR Analysis. Q-PCR analysis was performed using the AB™ 7500 Fast Real-Time PCR system (Applied Biosystems) as previously described (30). The following genes were analyzed using TaqMan Gene Expression assays; *MYB* (Hs00920554_m1, exons 1–2; Hs00193527_m1 exons 14–15), *API5* (Hs00362482_g1), *BCL2* (Hs00608023_m1), *BIRC3* (Hs00154109_m1), *CCNB1* (Hs00259126_m1), *CD34* (Hs00156373_m1), *CD53* (Hs00174065_m1), *CDC2* (Hs00364293_m1), *FGF2* (Hs00266645_m1), *HSPA8* (Hs01683591_g1), *KIT* (Hs00922211_m1), *MAD1L1* (Hs00269119_m1), *MYC* (Hs00153408_m1), *SET* (Hs00853870_g1), *VEGFA* (Hs00173626_m1), *TFEC* (Hs00232612_m1), and *CBX4* (Hs00186344_m1) (Applied Biosystems). All samples were assayed in triplicate. The relative expression levels of all genes were calculated using the comparative C_T method (ΔΔCt) (31) and the SDS Software v1.3.1 (Applied Biosystems) using the housekeeping genes *18S* (Hs99999901_s1) or GAPDH (Hs99999905_m1) as endogenous controls and cDNA from normal salivary gland tissue as the calibrator. Statistical analyses, including 2-tailed Wilcoxon signed rank test and 2-tailed Mann–Whitney *U* test, were performed using the GraphPad Prism 4 software (GraphPad Software).

Immunohistochemistry. For immunohistochemistry, paraffin sections from 5 ACCs were treated as previously described (32) and were incubated overnight at 4° C with a monoclonal MYB antibody (Abcam). Bound antibodies were visualized using the indirect immunoperoxidase technique with the DAKO EnVision+™ System (DakoCytomation). Control sections were incubated identically, except for the primary antibody, which was replaced by normal rabbit serum/mouse IgG.

Expression and Transfection of miRNAs. Total RNA, including miRNA, was extracted from fresh-frozen tumor samples (ACC3 and -5) and from frozen normal salivary gland tissue using the *mir*Vana™ miRNA isolation kit (Ambion). Normal human breast total RNA including miRNA was purchased from Ambion. We reverse transcribed 50 ng of each of the RNAs using the TaqMan MicroRNA Reverse Transcription Kit (Applied Biosystems) and RT-primers specific for miR-15a/16 and miR-150. To reverse transcribe the endogenous

controls, a small amount of random primer (1:4) was added to each reaction. Q-PCR analysis was performed in triplicate using TaqMan MicroRNA assays (Applied Biosystems) for hsa-miR-15a (assay ID: 000389), hsa-miR-16 (assay ID: 000391), and hsa-miR-150 (assay ID: 000473) according to the manufacturer's instructions. The relative expression levels of all miRNAs were calculated using the comparative C_T method ($\Delta\Delta$Ct) (31) and the SDS Software v1.3.1 (Applied Biosystems) using the housekeeping gene *18S* (Hs99999901_s1) as endogenous control and cDNA from normal salivary gland tissue as the calibrator.

MOLT-4 cells and primary cultured fusion-positive ACC cells from ACC2 and -6 were transfected with the premiR™ miRNA precursor molecules (Ambion) hsa-mir-15a (PM10235), hsa-mir-16 (PM10339), and hsa-mir-150 (PM10070) using the siPORT ™ *NeoFX* ™ Transfection Agent (AM4511) (Ambion). The PremiR™ miRNA Starter Kit was used for optimization, and a Cy™3-labeled PremiR™ miRNA precursor molecule (Ambion) was used as a control for transfection efficiency.

ACKNOWLEDGMENTS. We thank Barbro Wedell and Malin Hagberg for technical assistance and Ulric Pedersen for help preparing the illustrations. This work was supported by grants from the Swedish Cancer Society, the IngaBritt and Arne Lundberg Research Foundation, the Assar Gabrielsson Research Foundation for Clinical Cancer Research, and the Sahlgrenska University Hospital Foundations.

1. Mitelman F, Johansson B, Mertens F (2007) The impact of translocations and gene fusions on cancer causation. *Nature Reviews Cancer* 7:233–245.
2. Tomlins SA, et al. (2007) Distinct classes of chromosomal rearrangements create oncogenic *ETS* gene fusions in prostate cancer. *Nature* 448:595–599.
3. Nordkvist A, Mark J, Gustafsson H, Bang G, Stenman G (1994) Non-random chromosome rearrangements in adenoid cystic carcinoma of the salivary glands. *Genes Chromosomes Cancer* 10:115–121.
4. El-Naggar AK, Huvos AG (2005) in *World Health Organization Classification of Tumours. Pathology and Genetics of Head and Neck Tumours*, eds Barnes L, Eveson JW, Reichart P, Sidransky D (IARC Press, Lyon, France), pp 254–258.
5. Ellis IO, et al. (2003) in *World Health Organization Classification of Tumours. Pathology and Genetics of Tumors of the Breast and Female Genital Organs*, eds Tavassoli FA, Devilee P (IARC Press, Lyon, France), pp 13–59, 277–279, 322–323.
6. Geurts JM, et al. (1998) Identification of *NFIB* as recurrent translocation partner gene of *HMGIC* in pleomorphic adenomas. *Oncogene* 16:865–872.
7. Qian F, Kruse U, Lichter P, Sippel AE (1995) Chromosomal localization of the four genes (*NFIA*, *B*, *C*, and *X*) for the human transcription factor nuclear factor I by FISH. *Genomics* 28:66–73.
8. Stenman G (2005) Fusion oncogenes and tumor type specificity—insights from salivary gland tumors. *Seminars in Cancer Biology* 15:224–235.
9. Enlund F, Persson F, Stenman G (2004) Molecular analyses of the candidate tumor suppressor gene, *PLAGL1*, in benign and malignant salivary gland tumors. *European Journal of Oral Sciences* 112:545–547.
10. Oh IH, Reddy EP (1999) The *myb* gene family in cell growth, differentiation and apoptosis. *Oncogene* 18:3017–3033.
11. Ramsay RG, Gonda TJ (2008) *MYB* function in normal and cancer cells. *Nature Reviews Cancer* 8:523–534.
12. Visel A, Thaller C, Eichele G (2004) GenePaint.org: An atlas of gene expression patterns in the mouse embryo. *Nucleic Acids Res* 32:552–556.
13. Dasgupta P, Reddy EP (1989) Identification of alternatively spliced transcripts for human c-myb: Molecular cloning and sequence analysis of human *c-myb* exon 9A sequences. *Oncogene* 4:1419–1423.
14. Roulet E, et al. (1995) Regulation of the DNA-binding and transcriptional activities of *Xenopus laevis NFI-X* by a novel C-terminal domain. *Mol Cell Biol* 15:5552–5562.
15. Sakura H, et al. (1989) Delineation of three functional domains of the transcriptional activator encoded by the *c-myb* protooncogene. *Proc Natl Acad Sci USA* 86:5758–5762.
16. Dubendorff JW, Whittaker LJ, Eltman JT, Lipsick JS (1992) Carboxy-terminal elements of *c-Myb* negatively regulate transcriptional activation *in cis* and *in trans*. *Genes Dev* 6:2524–2535.
17. Press RD, Reddy EP, Ewert DL (1994) Overexpression of C-terminally but not N-terminally truncated *Myb* induces fibrosarcomas: A novel nonhematopoietic target cell for the *myb* oncogene. *Mol Cell Biol* 14:2278–2290.
18. Xiao C, et al. (2007) MiR-150 controls B cell differentiation by targeting the transcription factor c-Myb. *Cell* 131:146–159.
19. Chung EY, et al. (2008) c-Myb oncoprotein is an essential target of the dleu2 tumor suppressor microRNA cluster. *Cancer Biology and Therapy* 7:1758–1764.
20. Lin YC, et al. (2008) c-Myb is an evolutionary conserved miR-150 target and miR-150/c-Myb interaction is important for embryonic development. *Mol Biol Evol* 25:2189–2198.
21. Zhao H, Kalota A, Jin S, Gewirtz AM (2009) The c-myb proto-oncogene and microRNA-15a comprise an active autoregulatory feedback loop in human hematopoietic cells. *Blood* 113:505–516.
22. Lahortiga I, et al. (2007) Duplication of the *MYB* oncogene in T cell acute lymphoblastic leukemia. *Nat Genet* 39:593–595.
23. Phuchareon J, Ohta Y, Woo JM, Eisele DW, Tetsu O (2009) Genetic profiling reveals cross-contamination and misidentification of 6 adenoid cystic carcinoma cell lines: *ACC2*, *ACC3*, *ACCM*, *ACCNS*, *ACCS* and *CAC2*. *PLoS One* 4:e6040.
24. Lee YS, Dutta A (2007) The tumor suppressor microRNA let-7 represses the *HMGA2* oncogene. *Genes Dev* 21:1025–1030.
25. Mayr C, Hemann MT, Bartel DP (2007) Disrupting the pairing between let-7 and Hmga2 enhances oncogenic transformation. *Science* 315:1576–1579.
26. Clappier E, et al. (2007) The C-MYB locus is involved in chromosomal translocation and genomic duplications in human T-cell acute leukemia (T-ALL), the translocation defining a new T-ALL subtype in very young children. *Blood* 110:1251–1261.
27. Lang G, White JR, Argent-Katwala MJ, Allinson CG, Weston K (2005) Myb proteins regulate the expression of diverse target genes. *Oncogene* 24:1375–1384.
28. Frierson HF, Jr, et al. (2002) Large scale molecular analysis identifies genes with altered expression in salivary adenoid cystic carcinoma. *Am J Pathol* 161:1315–1323.
29. Patel KJ, Pambuccian SE, Ondrey FG, Adams GL, Gaffney PM (2006) Genes associated with early development, apoptosis and cell cycle regulation define a gene expression profile of adenoid cystic carcinoma. *Oral Oncology* 42:994–1004.
30. Persson F, et al. (2008) High-resolution array CGH analysis of salivary gland tumors reveals fusion and amplification of the FGFR1 and PLAG1 genes in ring chromosomes. *Oncogene* 27:3072–3080.
31. Livak KJ, Schmittgen TD (2001) Analysis of relative gene expression data using real-time quantitative PCR and the 2(-$\Delta\Delta$ C(T)) method. *Methods* 25:402–408.
32. Behboudi A, et al. (2006) Molecular classification of mucoepidermoid carcinomas-prognostic significance of the *MECT1-MAML2* fusion oncogene. *Genes Chromosomes Cancer* 45:470–481.